

## Ultrasonic Study of Three-Phonon Interactions. II. Experimental Results\*

FRED R. ROLLINS, JR., LYLE H. TAYLOR, AND PAUL H. TODD, JR.

*Midwest Research Institute, Kansas City, Missouri*

(Received 15 June 1964)

The intersection of two pulsed ultrasonic beams in isotropic solids is described as an experimental technique capable of yielding direct evidence of certain three-phonon interaction effects. It is shown that a third beam of reasonable intensity is generated at the volume of interaction only when energy and momentum are conserved between the three beams. Polarization effects and beam intensity relationships are in agreement with theoretical predictions. The four-phonon interaction is also examined by ultrasonic techniques, and the process is shown to be much weaker than the three-phonon interaction.

### I. INTRODUCTION

THE theoretical arguments set forth<sup>1</sup> in Paper I and a previous paper by Jones and Kobett<sup>2</sup> have formed the basis of an experimental program in which ultrasonic beams have been used to study three-phonon interactions in isotropic solids.

The theories indicate that three-phonon interactions are virtually forbidden except in those circumstances where energy and momentum are both conserved between the interacting phonons. An earlier paper<sup>3</sup> reported our preliminary findings that ultrasonic waves could be utilized in studying the nonlinear interaction phenomenon when the conservation conditions are satisfied. This paper provides details of the experimental arrangements together with additional results. Where possible, the experimental results are compared with theory.

It was pointed out in Paper I that our interest has been primarily limited to the interaction of ultrasonic beams that are not collinear. The interaction of collinear longitudinal phonons is of course theoretically predicted, and observation of such interactions has been recently reported by Shiren.<sup>4</sup> A somewhat related topic is the waveform distortion, or generation of harmonic components due to the propagation of finite amplitude ultrasonic waves. This phenomenon has also been observed in solids recently by a number of investigators.<sup>5,6</sup>

### II. EXPERIMENTAL ARRANGEMENTS

The block diagram of Fig. 1 shows a typical experimental setup that is quite useful in studies of the interaction phenomena. Disk-shaped specimens are prepared

with small "flats" machined at appropriate points along the circumference so that piezoelectric transducers may be bonded directly to the specimen. Quartz transducers (*X* cuts and *AC* cuts) have been used exclusively in this investigation with a wide variety of bonding agents. For a particular interaction, the flats are located such that energy and momentum are conserved between the three interacting waves. The two primary transducers (*A* and *B*) are driven by separate rf pulse generators. The two generators may be pulsed simultaneously or the variable delay may be used to provide a known time delay between the two pulses. The latter is necessary whenever transducers *A* and *B* are of dissimilar cut such that one produces a longitudinal beam and the other, a transverse or shear beam. If transducer *A* produces the shear beam and *B* produces a longitudinal beam, the pulsing of *B* must be delayed in order for the slower shear wave to intersect the faster longitudinal wave packet.

Transducer *C* is used to detect the wave that is generated by nonlinear interaction of the two primary beams. It is selected by frequency and mode to match the expected third-beam characteristics. The transducer output is fed through a tunable amplifier and displayed as a rectified pulse on the scope.

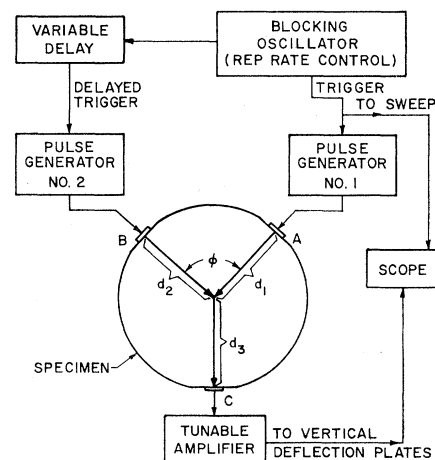


FIG. 1. Arrangement for observing interaction of ultrasonic beams.

\* Supported by the U. S. Air Force Materials Laboratory, Wright-Patterson Air Force Base, Ohio.

<sup>1</sup> Lyle Taylor and F. R. Rollins, Jr., preceding paper, *Phys. Rev.* **136**, A591 (1964).

<sup>2</sup> G. L. Jones and D. R. Kobett, *J. Acoust. Soc. Am.* **35**, 5 (1963).

<sup>3</sup> F. R. Rollins, Jr., *Appl. Phys. Letters* **2**, 147 (1963).

<sup>4</sup> N. S. Shiren, *Phys. Rev. Letters*, **11**, 3 (1963).

<sup>5</sup> A. A. Gedroits and Krasil'nikov, *Zh. Eksperim. i Teor. Fiz.* **43**, 1592 (1962) [English transl.: *Soviet Phys.—JETP* **16**, 1122 (1963)].

<sup>6</sup> M. A. Breazeale and D. O. Thompson, *Appl. Phys. Letters* **3**, 77 (1963).

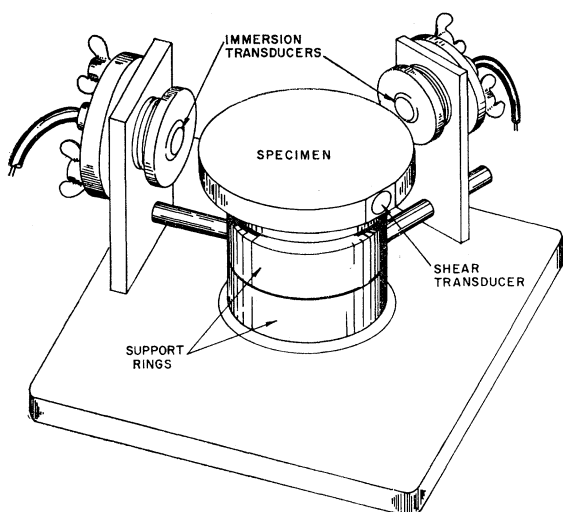


FIG. 2. Variable angulation apparatus for studying conservation conditions and beam spread.

There are a number of ways in which the detected pulse can be identified as originating at the intersection volume. First, the time of arrival of the signal at transducer *C* corresponds to acoustic propagation along path  $d_1$  and  $d_2$ . This time can be calculated from the known propagation velocities and can be measured with the calibrated sweep of the oscilloscope. In addition, the detected signal amplitude is greatest when the variable delay is adjusted to the calculated value necessary to produce simultaneous arrival of the two primary beams at the point of intersection.

Bonding of transducers directly to the specimen, as just described, has a number of advantages but it has serious limitations relative to studies of conservation conditions. Investigations of angulation and collimation characteristics of the interaction phenomenon have been greatly facilitated through the use of the apparatus shown in Fig. 2. This "ultrasonic goniometer" was designed specifically for interaction experiments in which one or two of the ultrasonic beams can be coupled into (or out of) the specimen through a liquid couplant. A 2½-in.-diam cylindrical shaft is mounted perpendicular to a heavy baseplate and the center of this shaft is an axis of rotation for two immersion-type transducers and the disk-shaped test specimen. Two transducer holders are attached to heavy rings that fit concentrically about the center shaft. The ring-shaft fit is very close, yet rotation of the rings about the shaft is smooth and easy. The transducer holders are equipped with alignment screws that work against pressure provided by heavy springs. The disk-shaped specimen is waxed onto a cap-like piece that fits snugly over the top of the shaft and also rotates about the shaft axis.

Figure 3 is a schematic presentation that illustrates the versatility of the above equipment. The specimen

is shown as a 6-in.-diam disk with a "flat" machined at position *A*. Shear-mode transducers can be bonded directly to this flat using either solid couplants such as Salol or viscous liquids such as Nonaq. The other two transducers (*B* and *C*) are immersion-type units. The central mounting shaft acts as an axis for the independent rotation of the two-immersion-type transducers as well as the disk-shaped specimen. The apparatus is partially submerged in a suitable liquid to provide coupling between the specimen and the immersion transducers. The arrows in Fig. 3 indicate the propagation vectors for a typical experiment; however, each transducer is interchangeable in its role as a transmitter or receiver. The angular positions of the specimen and the two immersion transducers are reproducible to better than one degree.

Most of our interaction experiments to date have been performed at frequencies between 5 and 50 Mc/sec. The quartz transducers are driven at their fundamental or odd-harmonic frequencies. Maximum power is delivered to the two primary transducers by impedance matching networks with each transducer in a parallel tank circuit that is electrically resonant at the mechanical frequency desired. Using arrangements of this type, several thousand volts (rms) can easily be applied to the transducers.

At the frequencies mentioned above, ultrasonic beams produced by transducers having diameters of  $\frac{1}{4}$ - $\frac{1}{2}$  in. are well collimated and are often treated as plane waves. Beam spreading does exist to some degree but has not been objectionable in the experiments discussed here.

### III. EXPERIMENTAL RESULTS

#### A. General

Let us consider the interaction of a 15-Mc longitudinal beam and a 10-Mc shear beam to produce a

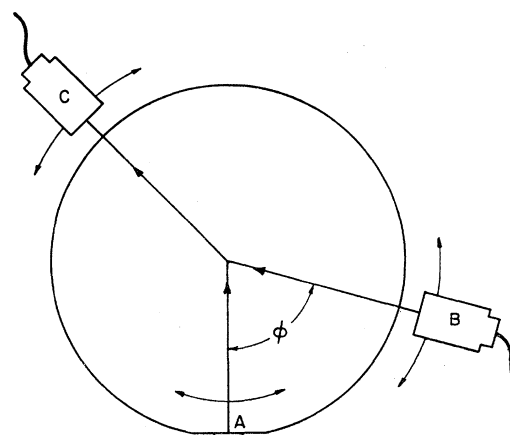


FIG. 3. Schematic presentation of variable angulation apparatus.

25-Mc longitudinal beam. We will denote such an interaction as follows:

$$L(15)+T(10) \rightarrow L(25).$$

The angular relationships for the interaction will depend on the specimen material but once the specimen is chosen it is an easy task to calculate<sup>1,2</sup> the required angle  $\phi$  between  $L(15)$  and  $T(10)$ . The propagation vector of the  $L(25)$  beam is simply the vector sum of the primary beam propagation vectors. When the transducers were appropriately located, interaction signals were successfully generated and detected in a variety of fused silica, polycrystalline aluminum, and polycrystalline magnesium specimens. All five interaction cases discussed in Paper I have been experimentally validated. Successful experiments have been performed with hundreds of different frequency and mode combinations where the conservation conditions are satisfied. However, negative results are always achieved when conservation conditions are intentionally avoided, or when the polarization of transverse waves is such that the interaction is theoretically forbidden.

### B. Beam Spread and Interaction Geometry

Using the apparatus shown in Fig. 2 several experiments have been performed to measure the "spread" or collimation characteristics of the scattered beam. The results indicate that the scattered beam is a relatively well-collimated signal with the peak intensity occurring at the theoretically predicted angle. In a rather typical experiment, conservation conditions were satisfied using the following interaction:

$$T(5)+T(5) \rightarrow L(10).$$

Interaction occurred at the center of a 6-in.-diam magnesium disk. The generated wave then traveled through 3 in. of magnesium, was coupled into water at the disk circumference, and was subsequently detected with an immersion transducer. The signal was observed as the transducer was rotated about an axis which passed through the interaction zone. The angular width of the beam at "half-peak amplitude" was approximately  $6^\circ$ . These results were obtained when the active area of the primary beam transducers was circular with a diameter of about 1 cm. When the two 5-Mc/sec transducers were driven at the third harmonic (15 Mc/sec), a scattered wave of 30 Mc/sec was detected, but the angular width at "half-peak amplitude" was then only about  $3^\circ$ . The increase in beam collimation is probably due to several factors including (1) better collimation and smaller relative band width of the primary beams at the higher frequency, and (2) increase in the ratio  $l/\lambda$  where  $l$  is the width of the interaction zone and  $\lambda$  is the wavelength of the scattered wave. The finite width of the interaction zone will produce some diffraction and consequent beam spread in the scattered wave. In the example given

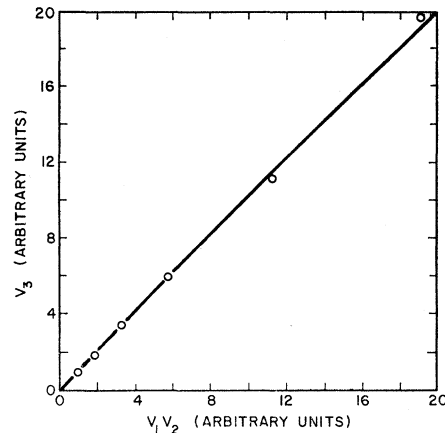


FIG. 4. Curve showing linear relationship between  $(V_1 V_2)$  and  $V_3$  where  $V_1$  and  $V_2$  are the voltages applied to the two primary transducers and  $V_3$  is the transducer voltage produced by the interaction wave.

above, the generated beam was probably still in a near-field configuration when it reached the transducer. Attempts to detect side lobes of this beam have not been successful even with the transducer much farther from the disk. Refraction at the curved solid-liquid boundary of course influences the character of the emerging wave and may have a tendency to "wash out" the side lobes.

In addition to studies of the angular spread of the scattered beam, the same apparatus of Fig. 2 has been used to explore the criticality of the interaction angle  $\phi$  between the two primary beams. Conservation conditions were first established in each case and then the angle between the two primary beams was varied on either side of the optimum angle until the amplitude of the scattered signal dropped to one-half amplitude. The total angular change  $\Delta\phi$ , to go from half-peak amplitude on one side of maximum interaction to half-peak amplitude on the other side was recorded. These values varied with frequency and the particular interaction geometry under study. It was generally between  $5$  and  $3^\circ$  with the more critical condition occurring at the higher frequencies.

### C. Amplitude of Interaction

The displacement amplitude of the generated beam should theoretically<sup>1,2</sup> be proportional to the product of the amplitudes of the two primary beams. This proportionality has been experimentally confirmed several times. It can be shown from piezoelectric equivalent circuit theory that when half-wave transducers are driven at resonance the displacement amplitude and voltage are linearly related. We see then that the voltage generated by the receiving transducer should be proportional to the product of the voltages applied to the two primary transducers. Figure 4 shows how closely this relationship is followed experimentally.

A more direct comparison of primary and generated

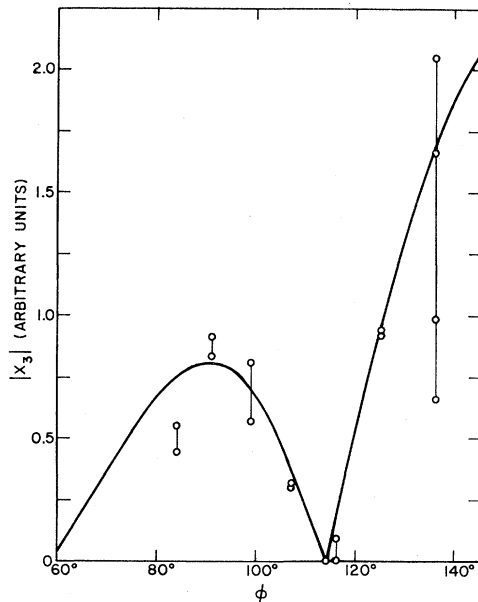


FIG. 5.  $|X_3|$  versus  $\phi$  for the interaction,  $L(\omega_1)+T(\omega_2) \rightarrow L(\omega_1+\omega_2)$ , showing experimental data (open circles) and normalized theoretical curve (solid line).

wave amplitudes has also been conducted in a variety of experiments. Displacement amplitudes have been calculated using equivalent circuit theory and the known voltages applied to the transducers. These calculated values are likely to be in error by several hundred percent from true amplitudes but they do permit qualitative comparisons. In a typical experiment, the displacement amplitude of a primary beam at 10 Mc/sec is about  $10^{-7}$  cm. Depending on the specimen material and mode of vibration, this value corresponds to a strain amplitude of about  $10^{-5}$ , or an ultrasonic beam intensity of approximately 1 W/cm<sup>2</sup>. The displacement amplitudes of the generated beams are generally nearer  $10^{-10}$  cm, about 60 dB weaker than the primaries. These values are in fair agreement with those calculated from the theory of interaction.<sup>1,2</sup> Quantitative comparison of the experimental and theoretical values has been hampered by a lack of third-order elastic constants for the materials we have been studying.

There are, however, several aspects of the interaction theory which can readily be compared with experimental results without knowledge of the third-order elastic constants. Equation (15) of Paper I, for example, gives the perturbing Hamiltonian for  $\alpha$ -type interactions ( $L \leftrightarrow T+T$ ). It is easily seen that the Hamiltonian goes to zero whenever one of the transverse waves is polarized parallel to the plane of interaction and the other transverse wave is polarized perpendicular to this plane. Likewise, one can see that for the  $\beta$ -type interactions ( $L \leftrightarrow L+T$ ) [see Eq. (16), Paper I] the Hamiltonian goes to zero whenever the single

transverse wave is polarized perpendicular to the plane of interaction. Both of these theoretical predictions have been experimentally confirmed in a number of experiments. In most such experiments the shear transducers were bonded to the specimens with viscous liquids (such as Nonaq stopcock grease) so the plane of polarization could be rotated while observing the amplitude of the scattered beam.

It was also pointed out in paper I that the  $\beta$ -type interactions go to zero whenever the longitudinal beams are perpendicular to each other. This purely geometrical feature occurs irrespective of the specimen material. This prediction has been confirmed experimentally using the interaction case III ( $L+T \rightarrow L$ ); the results are shown in Fig. 5. The open circles represent experimental data points. Since direct bonding techniques were employed in this experiment, transducers had to be replaced for each interaction requiring a different angle  $\phi$ . The interaction at a given angle was repeated at least twice and the scatter in these data is primarily due to variations in the transmission characteristics of the transducer bond. A completely quantitative comparison with theory is not possible because the third-order constants of the specimen (polycrystalline magnesium) are not available from an independent experiment. However, in the interaction case under discussion the elastic constants of the material enter into the calculations only as a multiplicative factor. It is, therefore, possible to normalize the theoretical curve (solid line) to the experimental data. The fit is quite good considering the problem of getting uniform and reproducible bonds. It is very clear that the interaction intensity does go to zero somewhere in the vicinity of the predicted angle.

(*Note added in proof.* Since the original submission of this paper, the third-order constants of polycrystalline magnesium have been determined in an independent experiment by R. T. Smith of Imperial College, London, and transmitted to the authors by private communication. These constants have been used to calculate the theoretically expected values of  $X_3$  for several different experimental conditions. Experimental values of  $X_3$  are always less than, but usually within an order of magnitude of the theoretical results. No attempt was made in these preliminary comparisons to correct for dissipative effects.)

The data of Fig. 5 were obtained using the rather laborious technique of bonding a different set of transducers to a different specimen geometry for each interaction. The ultrasonic goniometer described earlier would be an ideal instrument for this type experiment if it could be equipped with flat response transducers capable of producing beam intensities of 0.1–1.0 W/cm<sup>2</sup>. The consequent ease of shifting frequency and interaction angles while maintaining constant input intensity would greatly facilitate gathering experimental data such as those shown in Fig. 5, and comparing the results with theoretical curves like those presented in Paper I. With improved methods of accurately deter-

mining  $X_1$ ,  $X_2$ , and  $X_3$ , both of the third-order constants  $A$  and  $B$  could be separately evaluated by performing only two independent interaction experiments.

#### D. The Four-Phonon Interaction

As previously discussed the three-phonon interaction is directly related to those terms in the elastic energy expression that are cubic in the particle displacements. Four-phonon interactions arise from terms that are quartic in displacement. It is generally conceded that the four-phonon interaction should be considerably weaker than the three-phonon interaction, but no direct evidence of such has been presented. The ultrasonic interaction techniques already described have been used to shed some light on this subject.

For a three-phonon interaction, the conservation criteria establishes a unique angular relationship between the three interacting phonons. We find, however, that in the four-phonon interaction a particular combination of phonons may interact under various geometrical conditions and still conserve energy and momentum. Two separate experiments have been performed as variations of the interaction:

$$T(\omega_1) + T(\omega_2) + T(\omega_3) \rightarrow L(\omega_1 + \omega_2 + \omega_3).$$

The geometry of interaction was selected in each case to conserve energy and momentum for the over-all interaction. In one case conservation was also established for the intermediate interaction:

$$T(\omega_1) + T(\omega_2) \rightarrow L(\omega_1 + \omega_2).$$

In this experiment, the  $L(\omega_1 + \omega_2)$  beam was easily detected but the  $L(\omega_1 + \omega_2 + \omega_3)$  beam was undetectable. The intensity of the  $L(\omega_1 + \omega_2)$  beam was approximately

60 dB below that of the primary beams, and from knowledge of the noise level in our receiver system it was estimated that the  $L(\omega_1 + \omega_2 + \omega_3)$  beam was at least 60 dB below that of the  $L(\omega_1 + \omega_2)$  beam.

In a second attempt to observe the four-phonon interaction, the three transverse beams were intersected at angles which satisfied the conservation laws for the overall interaction but not for any intermediate interactions. Results were again negative.

The experiment described above is of considerable interest and value even though the  $L(\omega_1 + \omega_2 + \omega_3)$  beam was never detected. It confirms theoretical predictions concerning the relative probabilities of three- and four-phonon interactions. Similar experiments at higher frequencies where the interaction probability is much greater might reveal a four-phonon interaction and permit estimates of the fourth-order elastic constants. Also, certain resonance conditions<sup>7</sup> may generate a  $L(\omega_1 + \omega_2 + \omega_3)$  beam which may be detectable.

#### IV. CONCLUSIONS

The experimental results described in this paper illustrate that ultrasonic beams in the low-megacycle range can be effectively utilized to study elastic wave interactions in isotropic solids. Many of the theoretical predictions concerning variations in interaction intensity have been experimentally confirmed and characteristics of the generated beam have been determined. These results and future work of this type at higher frequencies in single crystals promise to be important in obtaining a more complete understanding of phonon-phonon interactions and the anharmonic elastic properties that give rise to such interactions.

<sup>7</sup> P. Carruthers, Phys. Rev. **125**, 123 (1962).